Preliminary Performance Test of STELLA-2 Reactor Vessel Cooling System

Seungjoon Baik*, Yong-Hoon Shin, Jung Yoon, In Sub Jun, Jewhan Lee
Korea Atomic Energy Research Institute, 989-111Dadeok-daero, Yuseong-gu, Daejeon, Korea
**Corresponding author: bsj227@kaeri.re.kr*

***Keywords :** Sodium cooled fast reactor, Reactor vessel cooling system, Liquid metal, Performance test, Thermal hydraulics

1. Introduction

Among Generation IV reactor systems, SFR (sodium-cooled fast reactor) has attracted attention as a practical power generation technology due to its high power density, high efficiency, and excellent inherent safety.

Due to its high thermal conductivity, sodium is an effective reactor coolant. In addition, its low melting point of 98 °C and high boiling point of 883 °C allow operation at elevated temperatures even under atmospheric pressure. In addition, when the primary coolant system of a reactor is designed as a pool-type rather than a loop-type configuration, enhanced safety can be achieved due to its large thermal capacity.

In pool-type reactors, decay heat can be removed to the surrounding air by utilizing the large surface area of the reactor vessel, and by employing passive mechanisms such as a chimney effect, no additional power is required. This approach is commonly referred to as RVACS (Reactor vessel auxiliary cooling system) or RVCS (Reactor vessel cooling system).

To investigate the air-cooling characteristics and decay heat removal performance of the RVCS applied to a sodium pool, performance tests were conducted using the STELLA-2 integral effect test facility located at the Korea Atomic Energy Research Institute [1, 2].

Figure 1 illustrates the RVCS configuration of the prototype reactor, PGSFR. The original concept consists of an inlet duct and a chimney; however, in STELLA-2, it was simplified into an air-jacket type, with air introduced by a blower without a chimney [3].

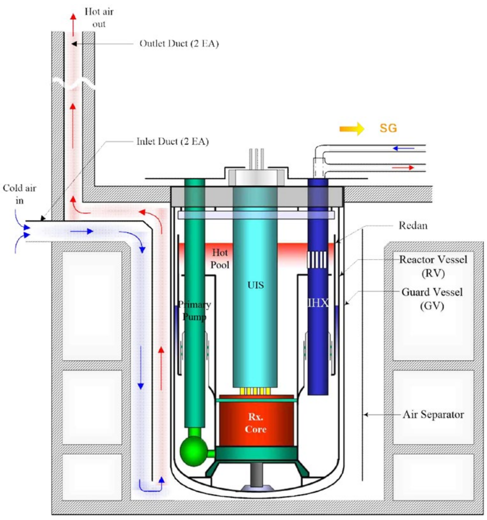

Fig. 1. Conceptual configuration of the RVCS in PGSFR.

2. Test facility and test methods

2.1. Description of STELLA-2 facility

The STELLA-2 test facility is a 1/5-length-scale integral effect test facility of the PGSFR. As shown in Figure 2, it consists of the PHTS (Primary heat transport system), IHTS (Intermediate heat transport system), DHRS (Decay heat removal system), and RVCS [3]. In this experiment, the PHTS and RVCS were used, while the IHTS and DHRS were isolated by valves to prevent energy inflow and outflow.

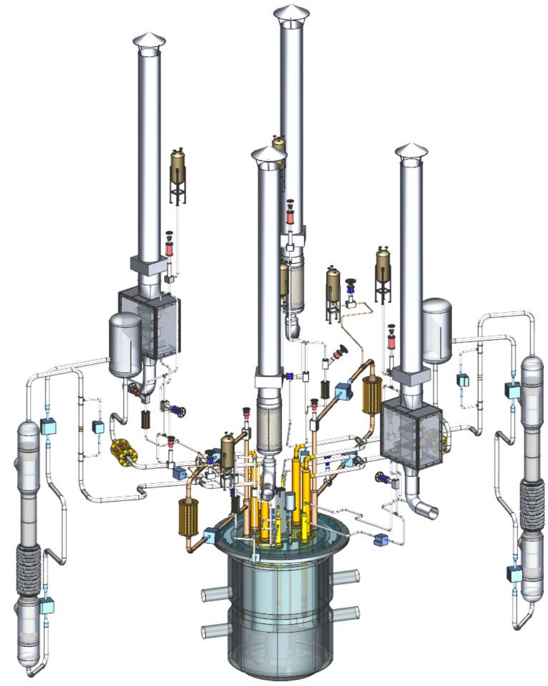

Fig. 2. STELLA-2 Facility layout

The RVCS consists of two air layers formed by an air-jacket surrounding the MRV (Model reactor vessel). The geometry and major parameters are shown in Figure 3 and Table I. All parts except the air layers are insulated with ceramic fiber (Cerak wool, KCC corporation), thicker than 150 mm, to minimize unwanted heat loss. The RVCS has two symmetrical inlets and outlets, with two blowers installed at the inlets, each rated at 300 m³/min and 500 mmAq. The air flow rate can be regulated by blower speed via inverters.

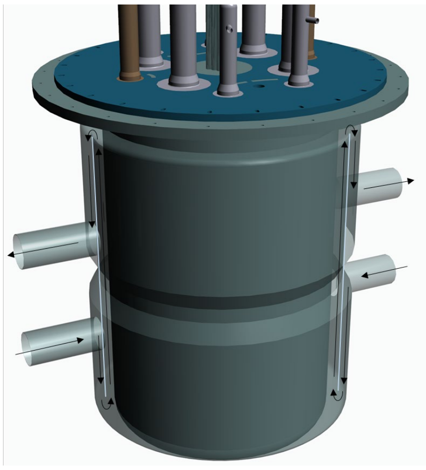

Fig. 3. STELLA-2 RVCS air jackets and flow directions.

Table I: Major geometric specifications of RVCS.

Component/Part		Parameter	Value	Note
MRV		Inner diameter	2130 mm	Wall thickness 10 mm
		Height	3260.4 mm	Cylindrical shell
		Lower plenum	436.3mm	Ellipsoidal head
RVCS	Piping	Inner diameter	310.5 mm	12" Sch. 10S
	Air jacket	Inner layer height	2902.8 mm	
		Inner layer Air gap	96 mm	Annulus
		Separator wall length	2703 mm	Wall thickness 2 mm
		Outer layer height	1366 mm	Lower and upper annulus
		Outer layer Air gap	100 mm	
Insulation		Thickness	150 mm	Ceramic fiber (Cerak wool)

2.2. Methods for system heat loss measurement

STELLA-2 is a large-scale integral effects test facility with multiple coupled systems, making it challenging to accurately quantify the heat removal rate solely through the RVCS. The relatively large uncertainty of the flow measurement at low flow rates is also attributed to this heat loss quantification difficulty.

Furthermore, it was found that a significant amount of heat was removed even when the RVCS airflow was completely blocked. Therefore, the authors classified this as one of the standby heat losses of STELLA-2.

By applying an empirical heat loss quantification method [4], individual heat loss components were characterized under steady-state heat balance conditions, as expressed in the following equations.

(1) $\Delta U = Q - W$

(2) $C\frac{dT}{dt} = \sum Q_{in} - \sum Q_{loss}$

(3) $C\frac{dT}{dt} = Q_{ECHB} + Q_{PSLS\,EMP} + Q_{Aux.heater} - (Q_{PSLS} + Q_{IHTS} + Q_{DHRS} + Q_{MRV} + Q_{RVCS})$

The energy equation of STELLA-2 was derived from the fundamental energy balance, and each term was listed in equation (3) to analyze the energy inflow and outflow.

The energy input to the system consists of the heat supplied to the core simulator (ECHB, Electric Core Heater Bundle), as well as contributions from the electromagnetic pump and auxiliary heaters on the primary pump simulation loops (PSLS). The energy contribution of the EMP (Electro Magnetic Pump) in the PSLS is neglected, as its power is relatively small and its external body is rather required to be cooled down in operation to prevent any damage to the electrical parts from overheating. The heat input from the auxiliary tracing heaters is also neglected, as they were not engaged during the experimental run.

Among the heat loss components listed in parentheses in equation (3), the objective of this study is to quantify the heat removal by the RVCS. As mentioned earlier, the RVCS removes heat even in the absence of airflow; therefore, as shown in equation (4), the RVCS heat removal is classified into standby and operation modes. Under steady-state conditions, the energy input required to maintain the system temperature was determined from the measured core simulator power. When the RVCS is in standby mode, the condition can be expressed as in equation (5), which corresponds to the standby heat loss of STELLA-2.

(4) $Q_{RVCS} = Q_{RVCS,stby} + Q_{RVCS,oper}$

(5) $\sum Q_{loss,stby} = Q_{PSLS} + Q_{IHTS} + Q_{DHRS} + Q_{MRV} + Q_{RVCS,stby}$

To quantify the heat removal by the RVCS in operation mode, the previously determined standby heat loss of STELLA-2 is subtracted from the core simulator power, as shown in equation (6). This value is then compared, as in equation (7), with the energy increase of the air calculated from the air-side.

(6) $Q_{RVCS,oper} = Q_{ECHB} - \sum Q_{loss,stby}$

(7) $Q_{RVCS,air} = \dot{m}C_p(T_{in} - T_{out})$

In addition, the heat removal rate of the RVCS can be expressed, as shown in Equation (8), as a function of the thermal–hydraulic and geometric parameters on both the heat source and sink sides.

(8) $Q_{RVCS} = f(T_{air}, \dot{m}_{\mathrm{RVCS}}, T_{PHTS}, \dot{m}_{\mathrm{PHTS}}, \ldots, \mathrm{Lv}_{\mathrm{pool}}, A_{MRV}, R_{MRV}, \varepsilon_{MRV}, \varepsilon_{RVCS})$

In this study, the primary variables related to RVCS performance were set as PHTS sodium temperature, sodium flow rate, and air flow rate. As described above, the RVCS performance tests were conducted under steady-state conditions maintaining the PHTS sodium temperature, while the core simulator power was recorded for each air flow rate.

The core simulator consists of nineteen 35-kW electric heaters, each controlled by an industrial power controller (PION-D3W-090-TP, Pion Eng.). The controller, which is a TPR (thyristor power regulator), monitors power in 0.1-kW increment based on the true-RMS method; therefore, the measurement uncertainty was assumed to be 1% of the full span.

The air flow rate of the RVCS was measured using a thermal mass flow meter (QuadraTherm 640i, Sierra Instrument), and its detailed specifications are provided in Table II. The temperatures of air and sodium were measured using Class 1 K-type thermocouples, with an accuracy of ±0.4% of the measured value or ±1.5 ℃, whichever is greater.

Table II: Instrumentation and Specifications.

Parameter	Flow rate	Temperature
Instrument Type	Thermal mass flow meter	Thermocouple
Model / Manufacturer	QuadraTherm 640i / Sierra Instrument	K-type Thermocouple / Wooju sensor
Range	0-5 kg/s	0~600 ℃
Accuracy	±0.75% Rdg +0.5% FS < 50% F.S / ±0.75% Rdg > 50% F.S	±1.5℃ or ±0.4%

2.3. Criteria for steady-state determination

As described above, the performance tests were conducted under steady state conditions by varying the PHTS temperature, the sodium flow rate, and the air side flow rate. Due to the large heat capacity of the facility and the relatively small energy exchange, it took a long time to establish the conditions and determine steady state. Therefore, to ensure a stable steady state, the system was permitted to stabilize for at least 30 minutes, and quasi-steady-state data were taken for 5 minutes after the conditions in Table III were verified. The acceptance criteria were established based on at least five times the system residence time and within twice the measurement uncertainty of the instruments.

In Table III, the core simulator power and RVCS inlet temperatures are not specified because these values vary depending on the experimental conditions. These dependent variables were also measured under steady-state conditions that met the acceptance criteria.

Table III: Steady state Acceptance Criteria

Measurement item	Reading requirement	Acceptance criteria
Core simulator power	-* kW	ΔP ≤ ±5.0 kW, Sustained for ≥ 5min
Cold pool temperature	350 / 450 ℃	ΔT ≤ ±3.0℃, Sustained for ≥ 5min
RVCS inlet temperature	-* ℃	
Air flowrate	0, 0.15, 0.3, 0.45, 0.6 kg/s	$\Delta\dot{m}$ ≤ ±0.1kg/s, Sustained for ≥ 5min

Note: *Value varies depending on experimental conditions

3. Test results

3.1. RVCS performance test results

The test results are summarized in Table IV. The experiments were conducted at 350 °C and 450 °C while varying the air side flow rate. The PHTS sodium flow rates were categorized as high flow condition (HF) and low flow condition (LF), corresponding to 20% and 2% of the PSLS pump power, respectively. The 2% pump power serves as the reference flow rate for transient experiments in STELLA-2, corresponding to a 7% scaled-down flow of the PGSFR [2]. Under low flow conditions, the elevated temperatures at the core outlet and hot pool affect the temperature distribution in the cold pool. In contrast, under high flow conditions (20%), the temperature in the cold pool remains uniform.

In these tests, the representative test metric was based on the mean temperature of the cold pool, measured at the central plane in the vertical direction.

Table IV: RVCS performance test results

Case	Pool temp. [℃]	PSLS pump [%]	Air flow rate [kg/s]	RVCS inlet temp. [℃]	RVCS outlet temp. [℃]	Note
350-HF	351.1	20	-	223.8	195.3	$Q_{loss, stby}$
	348.6	20	0.13	15.2	241.3	
	349.7	20	0.29	14.0	179.2	
	349.6	20	0.46	13.7	147.1	
	351.4	20	0.63	13.6	128.3	
350-LF	348.7	2	-	200.9	211.7	$Q_{loss, stby}$
	348.8	2	0.08	14.9	259.0	
	348.6	2	0.30	13.0	190.8	
	348.8	2	0.48	12.5	145.2	
	349.6	2	0.66	12.4	120.1	
450-HF	455.9	20	-	306.0	288.5	$Q_{loss, stby}$
	454.5	20	0.05	55.2	364.8	
	450.7	20	0.28	14.9	259.2	
	453.6	20	0.44	14.4	210.5	
	453.5	20	0.62	14.4	184.9	
450-LF	456.2	2	-	303.5	285.6	$Q_{loss, stby}$
	453.1	2	0.03	35.1	371.3	
	452.7	2	0.27	20.5	303.5	
	453.3	2	0.43	15.8	236.8	
	454.4	2	0.61	14.6	193.0	

The air flow rates listed in Table IV represent the sum of the flows measured at the two inlets.

Cases with no air flow correspond to the standby condition, in which the core simulator power reflects the system heat loss. Under this condition, with no air-side flow, the inlet temperature rises and in some cases remain higher than the outlet temperature.

3.2. Comparison and analysis of experimental results

The RVCS-related heat quantities expressed in equations (6) and (7) in Section 2.2 are presented and compared in Table V. It can be observed that the heat removal rate increases with increasing airflow and with higher PHTS temperatures. However, variations in the heat removal characteristics versus PHTS flow were not significant.

Table V: RVCS performance test results comparison

Case	Air flow rate [kg/s]	Core simulator power [kW]	$Q_{RVCS, oper}$ [kW]	$Q_{RVCS, air}$ [kW]	Difference [kW]	Note
350-HF	-	51.2	-	-	-	$Q_{loss, stby}$
	0.13	75.7	24.5	29.4	-4.9	
	0.29	86.2	35.0	48.2	-13.2	
	0.46	100.1	48.9	62.0	-13.1	
	0.63	114.0	62.7	72.5	-9.8	
350-LF	-	58.3	-	-	-	$Q_{loss, stby}$
	0.08	75.7	17.4	20.5	-3.1	
	0.30	96.7	38.3	54.5	-16.2	
	0.48	110.6	52.2	64.2	-11.9	
	0.66	120.9	62.5	71.9	-9.3	
450-HF	-	65.3	-	-	-	$Q_{loss, stby}$
	0.05	86.2	20.9	15.8	5.1	
	0.28	117.5	52.2	69.4	-17.2	
	0.44	145.3	80.0	88.1	-8.1	
	0.62	169.6	104.4	106.4	-2.1	
450-LF	-	65.2	-	-	-	$Q_{loss, stby}$
	0.03	93.1	27.9	11.3	16.6	
	0.27	128.0	62.8	77.0	-14.2	
	0.43	155.7	90.5	96.4	-5.9	
	0.61	183.5	118.3	110.2	8.1	

Figure 4 plots the relationship between the heat quantities defined in equations (6) and (7). With acceptable discrepancies, this approach was found to be suitable for quantifying heat losses and analyzing the heat removal characteristics of the RVCS in an integral thermal–hydraulic test facility with large uncertainties. Measures to reduce uncertainty will be explored in future work.

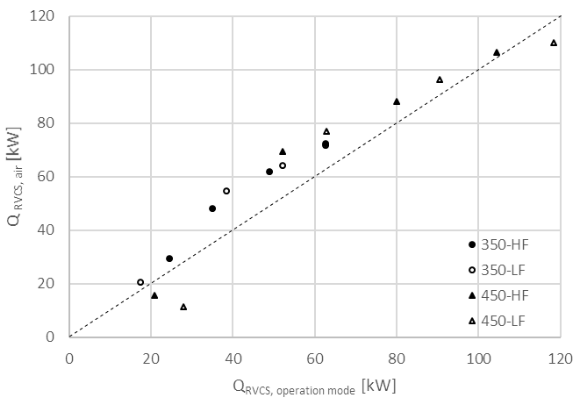

Fig.4. Comparison of two RVCS heat removal quantification methods

4. Conclusion and further works

A preliminary performance evaluation test was conducted to assess the RVCS performance and cooling characteristics of STELLA-2. It was confirmed that heat removal is effective due to the relatively large surface area of the pool-type reactor. Cooling was found to increase with higher temperatures and greater air flow, and heat removal by the RVCS was observed even under conditions with no air flow. This was classified as standby mode heat loss to estimate the RVCS heat removal during operation.

To evaluate RVCS heat removal, the energy supplied on the sodium side of the reactor vessel was compared with the energy received on the air side. Despite the difficulty in distinguishing system-level and component-level heat removal due to the characteristics of the integral test facility, the proposed method was confirmed to be suitable.

Uncertainty analyses for each method will be conducted to reduce measurement uncertainty. To understand the heat transfer mechanisms of the RVCS under standby and operational conditions, modeling and analysis will be conducted using a 1D system code. Future work will include transient experiments and comparisons with code simulation results to evaluate the RVCS characteristics and their impact on the primary reactor cooling system.

ACKNOWLEDGEMENT

This work was supported by the National Research Foundation of Korea (NRF) grant funded by the Korea government (MSIT). (No. RS-2025-16012975)

REFERENCES

[1] J. Lee et al., "Design evaluation of large-scale sodium integral effect test facility (STELLA-2) using MARS-LMR", Annals of Nuclear Energy, Vol. 120, pp.845-856, 2018.

[2] J. Eoh, "Engineering Design of Sodium Thermal-hydraulic Integral Effect Test Facility (STELLA-2)", KAERI SFR Design Report, SFR-720-TF-462-002 Rev.00, 2015.

[3] Y. Shin et al., " Modeling Specifications for System Code Analysis of the STELLA-2 Sodium Integral Effects Test Facility" KAERI/TR-11510/2026. 2026.

[4] J. Sanders, "Methods of heat loss measurement for a thermohydraulic facility" Experimental Heat Transfer, vol. 4, pp.127-151, 1991.